

# Modeling Identification and Control of Affordable UAVs

Dr. Mihai Huzmezan

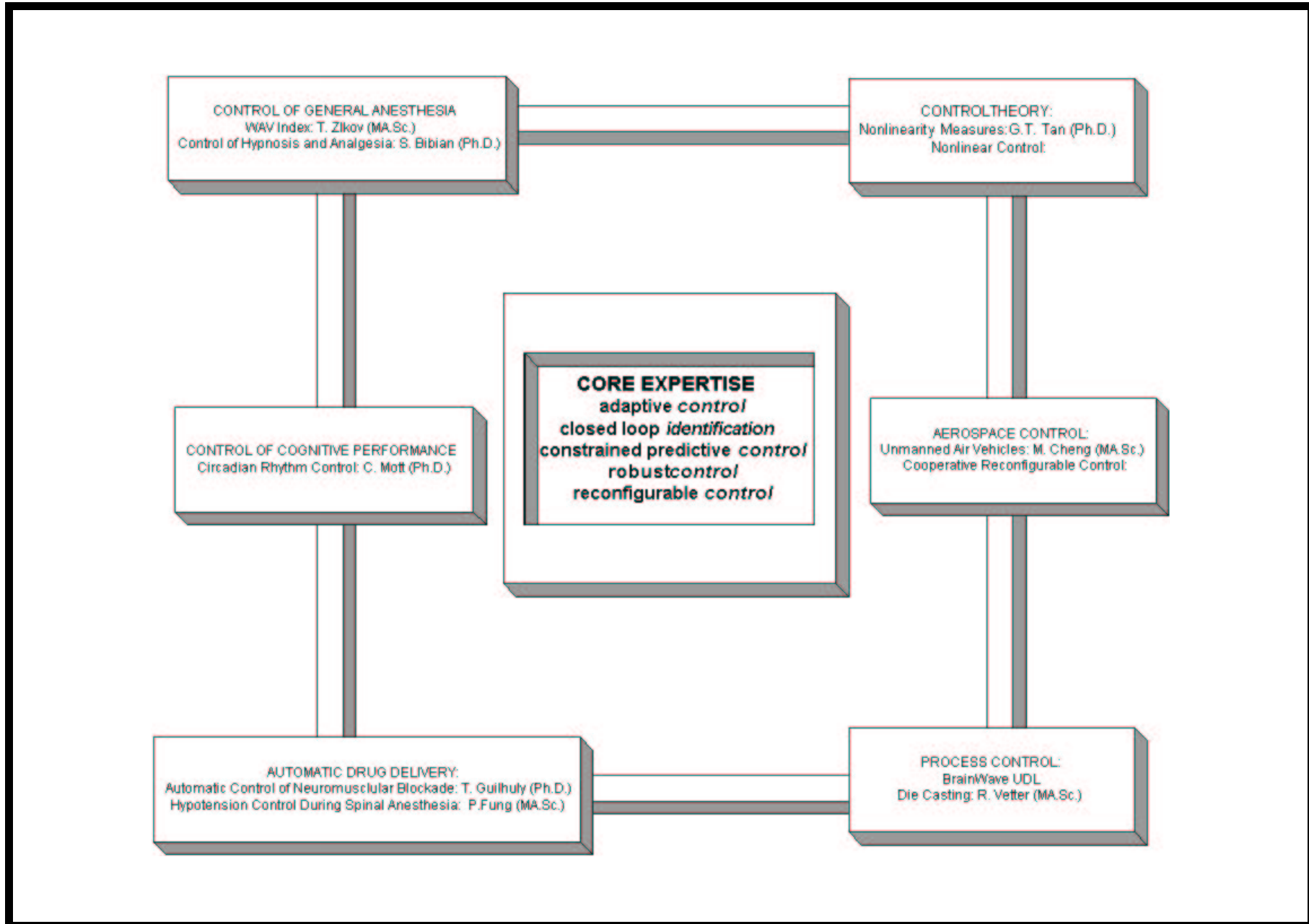
[huzmezan@ece.ubc.ca](mailto:huzmezan@ece.ubc.ca)

University of British Columbia  
Electrical and Computer Engineering



## Talk Overview

- The UAV rig
- The UAV model
- The Quasi-Linear Parameter Varying model
- A closed loop nonlinearity measure
- Controller architecture and performance
- Conclusions
- Future Work



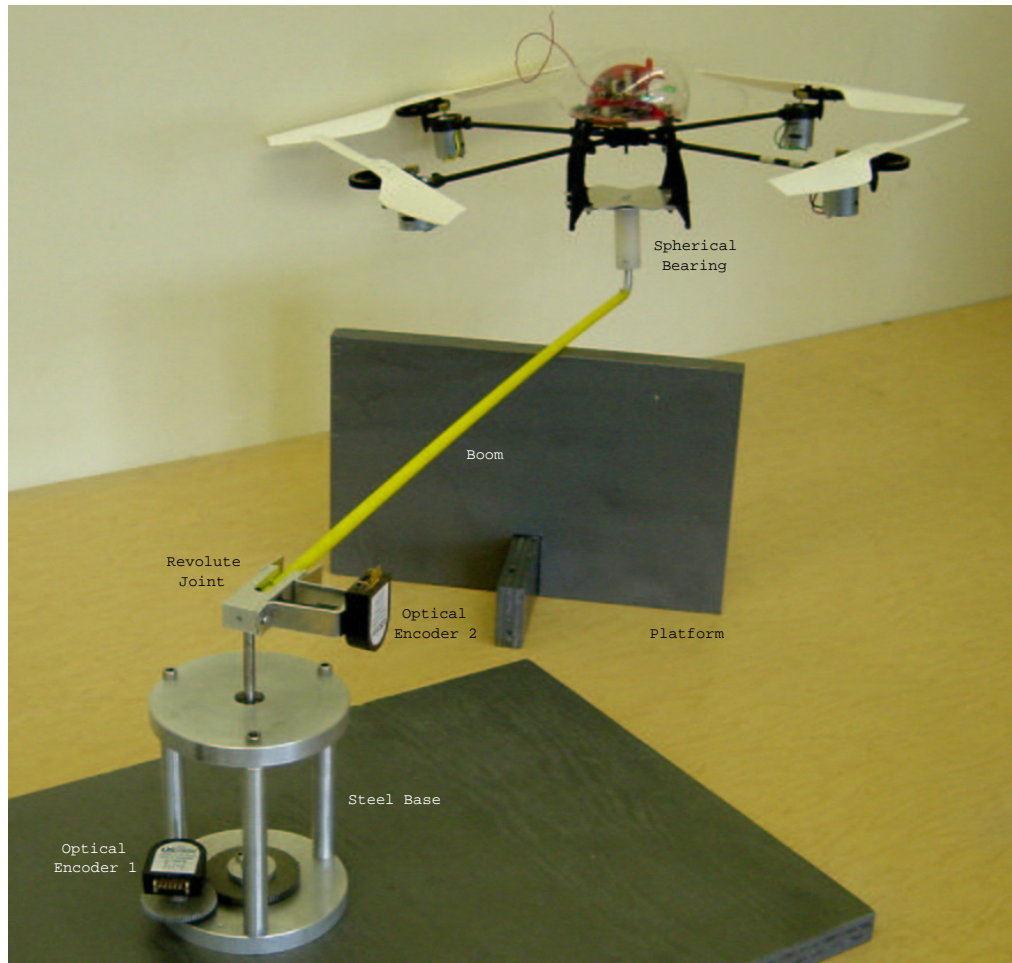
## **Advantages of Quad-rotor UAVs**

- Used to perform intelligence, surveillance and reconnaissance missions.
- Higher maneuverability (vertical take-off and landing and higher accelerations) for urban missions.
- Cost effective versus manned aircrafts.
- Little human intervention hence no potential loss of lives.

## **Scope of this project**

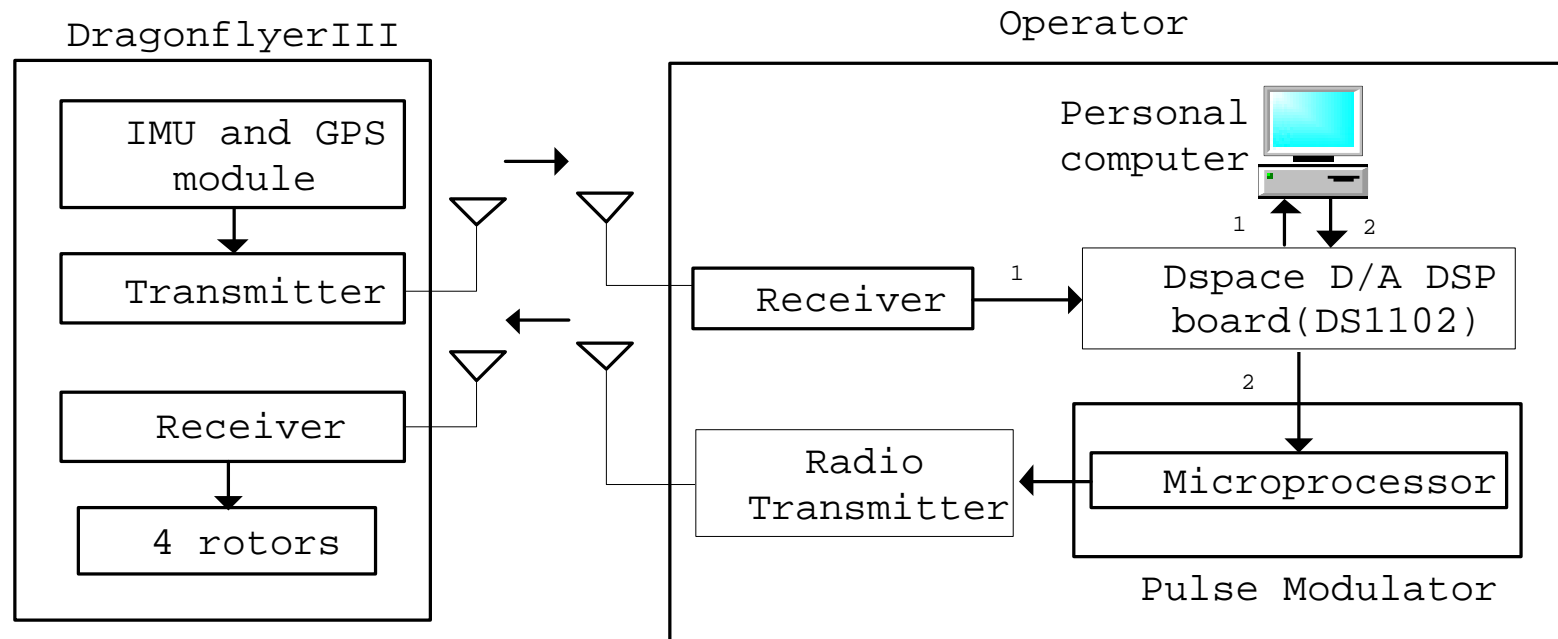
- Quad-rotor helicopter modelling and identification.
- UAV sensor integration.
- Robust control laws design and implementation.
- Geared towards a proof of concept for formation flying and cooperation control.

## The UAV and Its Experimental Flying Mill



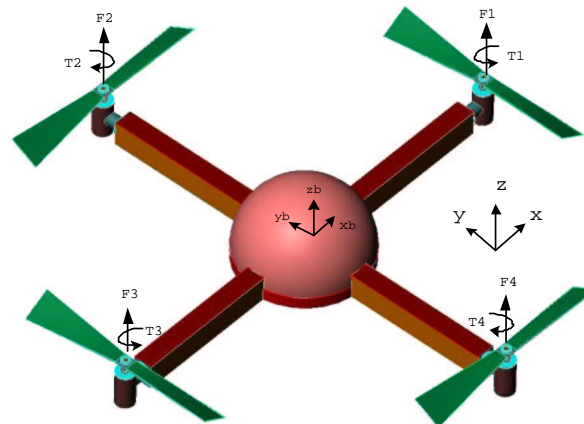
- A commercial flying model is used as starting point.
- For identification and control testing, a flying mill was built.
- The UAV is instrumented with DGPS, 3 axis accelerometers and gyros.

## Data Flow in the Experimental System



## Motion Equations of the Quad-rotor UAV (I)

Symbol	Definition
$u(1)$	$u(1) = F_1 + F_2 + F_3 + F_4$
$u(2)$	$u(2) = F_4 - F_2$
$u(3)$	$u(3) = F_3 - F_1$
$u(4)$	$u(4) = F_1 - F_2 + F_3 - F_4$
$F_{xB}, F_{yB}, F_{zB}$	force in body-axis x,y,z direction
$F_x, F_y, F_z$	force in earth-axis x,y,z direction
$I_x, I_y, I_z$	moment of inertia in x,y,z direction
$p, q, r$	roll rate, pitch rate, yaw rate
$\phi, \theta, \psi$	roll angle, pitch angle, yaw angle
$u_B, v_B, w_B$	velocity in body-axis x,y,z direction
$u, v, w$	velocity in earth-axis x,y,z direction
$x, y, z$	COG in earth-axis x,y,z direction



## Motion Equations of the Quad-rotor UAV (II)

Using the rotational transformation matrix

$$\begin{bmatrix} \cos \psi \cos \theta & -\sin \psi \cos \phi + \cos \psi \sin \theta \sin \phi & \sin \psi \sin \phi + \cos \psi \sin \theta \cos \phi \\ \sin \psi \cos \theta & \cos \psi \cos \phi + \sin \psi \sin \theta \sin \phi & -\cos \psi \sin \phi + \sin \psi \sin \theta \cos \phi \\ -\sin \theta & \cos \theta \sin \phi & \cos \phi \cos \theta \end{bmatrix}$$

The forces acting on the UAV in the earth-fixed frame are

$$\begin{bmatrix} F_x \\ F_y \\ F_z \end{bmatrix} = \left( \sum_{i=1}^4 F_i \right) \begin{bmatrix} \sin \psi \sin \phi + \cos \psi \sin \theta \cos \phi \\ -\cos \psi \sin \phi + \sin \psi \sin \theta \cos \phi \\ \cos \phi \cos \theta \end{bmatrix}$$

## Motion Equations of the Quad-rotor UAV (III)

The equations of motion are:

$$m \begin{bmatrix} \ddot{x} \\ \ddot{y} \\ \ddot{z} \end{bmatrix} = \begin{bmatrix} \sum_{i=1}^4 F_i (\sin \psi \sin \phi + \cos \psi \sin \theta \cos \phi) - K_1 \cdot \dot{x} \\ \sum_{i=1}^4 F_i (\sin \psi \sin \theta \cos \phi - \cos \psi \sin \phi) - K_2 \cdot \dot{y} \\ \sum_{i=1}^4 F_i \cos \phi \cos \theta - mg - K_3 \cdot \dot{z} \end{bmatrix}$$

$$\ddot{\phi} = l(F_3 - F_1 - K_4 \dot{\phi})/I_x$$

$$\ddot{\theta} = l(F_4 - F_2 - K_5 \dot{\theta})/I_y$$

$$\begin{aligned} \ddot{\psi} &= (M_1 - M_2 + M_3 - M_4 - K_6 \dot{\psi})/I_z \\ &= (F_1 - F_2 + F_3 - F_4 - K'_6 \dot{\psi})/I'_z \end{aligned}$$

$M_i$  – the moments of rotor  $i$ ;

$I'_z$  – the z axis moment of inertia and the force to moment scaling factor;

$m$  – the UAV mass;

## Motion Equations of the Quad-rotor UAV (IV)

For compatibility with the radio transmitter, the inputs are defined as:

$$\begin{aligned} u(1) &= F_1 + F_2 + F_3 + F_4 & u(3) &= F_3 - F_1 \\ u(2) &= F_4 - F_2 & u(4) &= F_1 - F_2 + F_3 - F_4 \end{aligned}$$

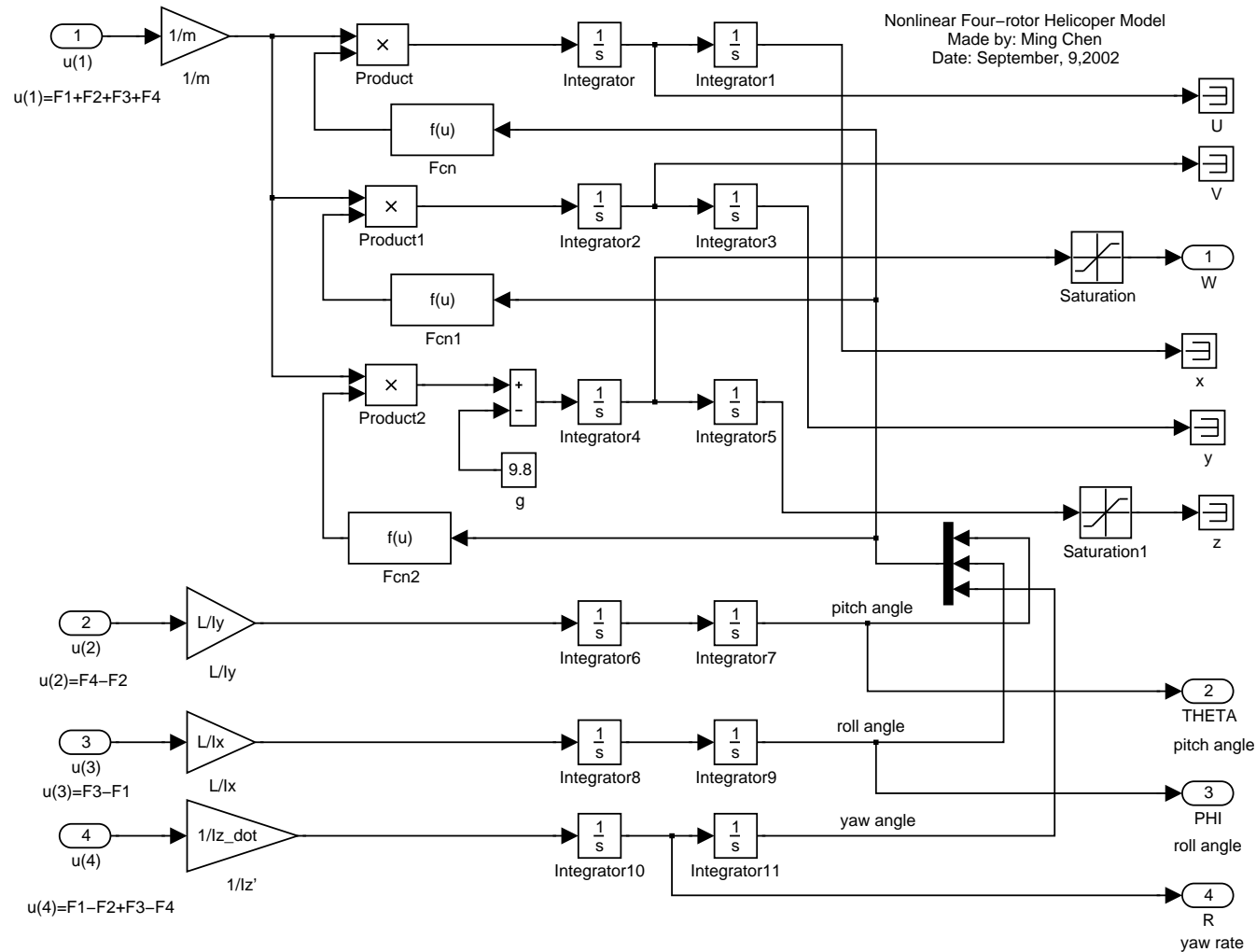
Hence the system model is:

$$\begin{aligned} \ddot{x} &= \frac{u(1)(\sin \psi \sin \phi + \cos \psi \sin \theta \cos \phi) - K_1 \cdot \dot{x}}{m} \\ \ddot{y} &= \frac{u(1)(\sin \psi \sin \theta \cos \phi - \cos \psi \sin \phi) - K_2 \cdot \dot{y}}{m} \\ \ddot{z} &= \frac{u(1) \cos \phi \cos \theta - K_3 \cdot \dot{z}}{m} - g \\ \ddot{\theta} &= (u(2) - K_5 \dot{\theta})l/I_y \\ \ddot{\phi} &= (u(3) - K_4 \dot{\phi})l/I_x \\ \ddot{\psi} &= (u(4) - K_6' \dot{\psi})/I_z' \end{aligned}$$

## Identification and Validation

- Parameters such as  $I_x, I_y$  and  $I_z$  for this model can be either measured or identified.
- Grey box identification, which keeps the model structure intact is used.
- The Quasi-LPV model form is preferred for grey box identification.
- Using the model, the drag coefficients  $K_{1-6}$  at low speeds were identified close to zero.

## Simplified Simulink Diagram of the Nonlinear Quad-rotor UAV Model



## High Fidelity Models Written in the Quasi-LPV Form (I)

- A Quasi-LPV model embeds the plant nonlinearities without interpolating between point-wise linearization.
- The Quasi-LPV approach is mostly suited for systems exhibiting state nonlinearities.
- The main characteristic of these models is that the scheduling variable is a state of the model.
- The nonlinear model is written in a form that the nonlinearities depend only on the scheduling variable  $\alpha$ :

$$\frac{d}{dt} \begin{bmatrix} \alpha \\ q \end{bmatrix} = f(\alpha) + \begin{bmatrix} A_{11}(\alpha) & A_{12}(\alpha) \\ A_{21}(\alpha) & A_{22}(\alpha) \end{bmatrix} \begin{bmatrix} \alpha \\ q \end{bmatrix} + \begin{bmatrix} B_{11}(\alpha) \\ B_{21}(\alpha) \end{bmatrix} \delta$$

where  $q$  are vectors of plant states not used for scheduling.

## The Quasi-LPV equations (II)

A family of equilibrium states, parametrised by the scheduling variable  $\alpha$ , is obtained by setting the state derivatives to zero:

$$0 = f(\alpha) + A(\alpha) \begin{bmatrix} \alpha \\ q_{eq}(\alpha) \end{bmatrix} + B(\alpha)\delta_{eq}(\alpha)$$

When it is impossible to embed all the system nonlinearities in the output then the model has to be approximated up to first order terms in all the states except the scheduling parameters.

### The Quasi-LPV equations (III)

Providing that there exist continuously differentiable functions  $q_{eq}(\alpha)$  and  $\delta_{eq}(\alpha)$ , we are able to write:

$$\frac{d}{dt} \begin{bmatrix} \alpha \\ q - q_{eq}(\alpha) \end{bmatrix} = \begin{bmatrix} 0 & A_{12}(\alpha) \\ 0 & A_{22} - \frac{d}{d\alpha} q_{eq}(\alpha) A_{12}(\alpha) \end{bmatrix} \begin{bmatrix} \alpha \\ q - q_{eq}(\alpha) \end{bmatrix} + \begin{bmatrix} B_{11}(\alpha) \\ B_{21}(\alpha) - \frac{d}{d\alpha} q_{eq}(\alpha) B_{11}(\alpha) \end{bmatrix} (\delta - \delta_{eq}(\alpha)) \quad (1)$$

### Remarks on the Quasi-LPV form

- The above form gives a different  $\alpha$ -dependent family than would be obtained by point-wise linearisation.
- To use the above system equations, the function  $\delta_{eq}(\alpha)$  must be known, not knowing it we need to estimate it by using an ‘inner loop’.
- Because of model uncertainty, this can reduce the robustness of the main control loop in a way which is difficult to predict at the design stage.
- The solution is simple, we avoid the problem generated by the existence of an inner loop required to compute  $\delta_{eq}(\alpha)$  by adding an integrator at the plant input.

## The Quasi-LPV equations (IV)

Following the addition of the input integrator the modified quasi-LPV is:

$$\frac{d}{dt} \begin{bmatrix} \alpha \\ q - q_{eq}(\alpha) \\ \delta - \delta_{eq}(\alpha) \end{bmatrix} = \begin{bmatrix} 0 & A_{12}(\alpha) & B_{11}(\alpha) \\ 0 & A_{22} - \frac{d}{d\alpha} q_{eq}(\alpha) A_{12}(\alpha) & B_{21}(\alpha) - \frac{d}{d\alpha} [q_{eq}(\alpha)] B_{11}(\alpha) \\ 0 & -\frac{d}{d\alpha} [\delta_{eq}(\alpha)] A_{12}(\alpha) & -\frac{d}{d\alpha} \delta_{eq}(\alpha) B_{11}(\alpha) \end{bmatrix} \times \quad (2)$$

$$\begin{bmatrix} \alpha \\ q - q_{eq}(\alpha) \\ \delta - \delta_{eq}(\alpha) \end{bmatrix} + \begin{bmatrix} 0 \\ 0 \\ 1 \end{bmatrix} \nu$$

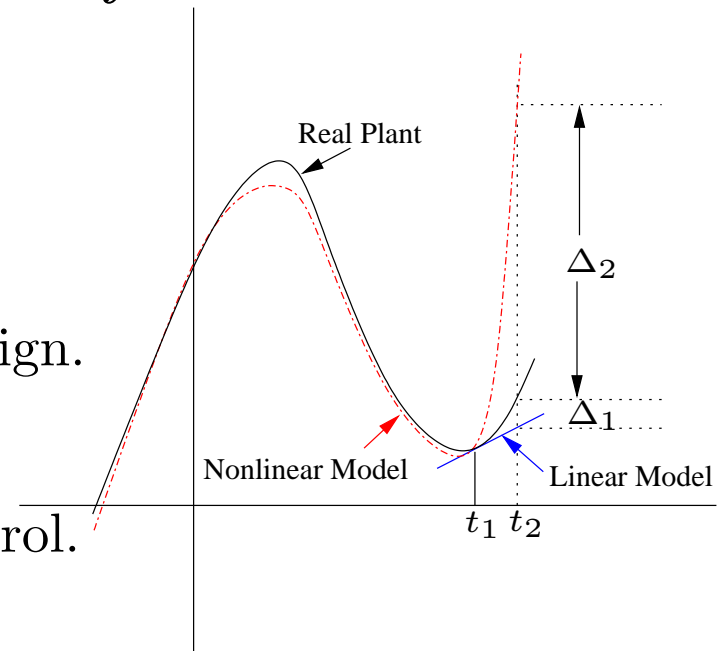
## The Simplified Quasi-LPV Form of the Quad-rotor UAV

$$\frac{d}{dt} \begin{bmatrix} \dot{x} \\ \dot{y} \\ \dot{z} \\ \dot{\theta} \\ \dot{\phi} \\ \dot{\psi} \\ g \\ \theta \\ \phi \\ \psi \end{bmatrix} = \begin{bmatrix} 0 & 0 & 0 & 0 & 0 & 0 & 0 & 0 & 0 & 0 \\ 0 & 0 & 0 & 0 & 0 & 0 & 0 & 0 & 0 & 0 \\ 0 & 0 & 0 & 0 & 0 & 0 & -1 & 0 & 0 & 0 \\ 0 & 0 & 0 & 0 & 0 & 0 & 0 & 0 & 0 & 0 \\ 0 & 0 & 0 & 0 & 0 & 0 & 0 & 0 & 0 & 0 \\ 0 & 0 & 0 & 0 & 0 & 0 & 0 & 0 & 0 & 0 \\ 0 & 0 & 0 & 0 & 0 & 0 & 0 & 0 & 0 & 0 \\ 0 & 0 & 0 & 1 & 0 & 0 & 0 & 0 & 0 & 0 \\ 0 & 0 & 0 & 0 & 1 & 0 & 0 & 0 & 0 & 0 \\ 0 & 0 & 0 & 0 & 0 & 1 & 0 & 0 & 0 & 0 \end{bmatrix} \begin{bmatrix} \dot{x} \\ \dot{y} \\ \dot{z} \\ \dot{\theta} \\ \dot{\phi} \\ \dot{\psi} \\ g \\ \theta \\ \phi \\ \psi \end{bmatrix} +$$

$$\begin{bmatrix} \frac{\sin \psi \sin \phi + \cos \psi \sin \theta \cos \phi}{m} & 0 & 0 & 0 \\ \frac{\sin \psi \sin \theta \cos \phi - \cos \psi \sin \phi}{m} & 0 & 0 & 0 \\ \frac{\cos \phi \cos \theta}{m} & 0 & 0 & 0 \\ 0 & l/I_y & 0 & 0 \\ 0 & 0 & l/I_y & 0 \\ 0 & 0 & 0 & I_z \\ 0 & 0 & 0 & 0 \\ 0 & 0 & 0 & 0 \\ 0 & 0 & 0 & 0 \\ 0 & 0 & 0 & 0 \end{bmatrix} \begin{bmatrix} u(1) \\ u(2) \\ u(3) \\ u(4) \end{bmatrix}$$

## Motivation For A Nonlinearity Measure

- Model fidelity is crucial to a good model based controller design.
- Intuitively, a nonlinear model is preferred for a nonlinear system design.
- The severity of nonlinearity influences the need for nonlinear control.
- A nonlinearity measure is required.



Previous work:

Statistical approach: Ramsey (1969), Brock et al. (1987)

Normed bounded approach: Nikolau (1993), Ogunnaike et al. (1993)

Geometrical approach: Vinnicombe (1993), Guay et al. (1995, 1997).

## The Nonlinearity Measure

- Ingredients of the proposed nonlinearity measure:
  - Quasi-LPV representation of a nonlinear system.
  - Knowledge on  $\mathcal{H}_\infty$  loop-shaping and the Vinnicombe metric.
- Characteristics:
  - Is an indirect nonlinearity assessment.
  - Exploits the special structure of the model.
  - Has strong connection with robust stability notion.

### The Vinnicombe's Metric

- The Vinnicombe's or  $\nu$  gap between two systems  $P_1$  and  $P_2$  is:

$$\delta_\nu(P_1, P_2) \triangleq \begin{cases} \|(I + P_2 P_2^*)^{-\frac{1}{2}} (P_1 - P_2) (I + P_1 P_1^*)^{-\frac{1}{2}}\|_\infty, & \text{if Index}(P_1, P_2) = 0 \\ 1, & \text{otherwise} \end{cases}$$

$$\text{Index}(P_1, P_2) \triangleq \eta(P_1, P_2^*) - \text{deg}(P_2).$$

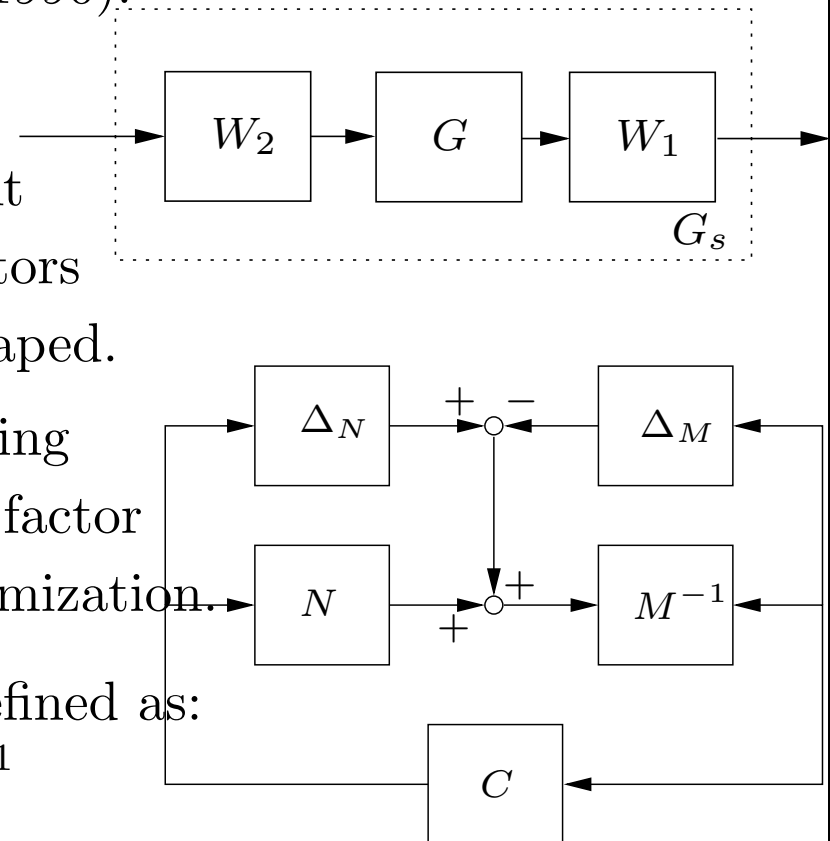
$\eta$  and  $\text{deg}$  denote the number of open RHP poles and McMillan degree, respectively.

- The  $\nu$  gap metric has a strong connection with the generalized stability margin and therefore the  $\mathcal{H}_\infty$  loop-shaping.

## $\mathcal{H}_\infty$ Loop-Shaping

- Is based on the  $\mathcal{H}_\infty$  robust stabilization and classical loop shaping (McFarlane and Glover, 1990).
- Consists of two steps:
  1. The shaping of open-loop plant using pre- and post-compensators to give a desired open-loop shaped.
  2. Robustly stabilizing the resulting shaped plant w.r.t to coprime factor uncertainty using an  $\mathcal{H}_\infty$  optimization.
- Generalized stability margin is defined as:

$$b_{PC} := \left\| \begin{bmatrix} C \\ I \end{bmatrix} (I - GC)^{-1} M^{-1} \right\|_\infty^{-1}$$



## $\nu$ -Gap and $\mathcal{H}_\infty$ Loop Shaping

- $\nu$ -gap metric quantifies the “closeness” of two linear plants with unity feedback. This is actually the radius of the uncertainty ball allowed for the perturbed plant.
- Generalized stability margin indicates how large the uncertainty that a given closed-loop system tolerates before becoming unstable.
- If  $b_{PC} > \delta_\nu$ , the uncertainty is manageable.
- If  $b_{PC} < \delta_\nu$ , the uncertainty is too large and the controller  $C$  can not cope with it.

## A Computational Algorithm (I)

1. Recast the nonlinear system into a Quasi-LPV representation.
2. Grid the scheduling parameter space. A set of linear models is then easily obtained by simply freezing the scheduling parameter.
3. For each model, the  $\nu$ -gaps to all other models are obtained:  

$$\delta_i = \{ \delta_\nu(x_i, x_j), \forall x_j \in \mathcal{X} \}$$
4. Choose  $G_0$ , the best nominal model for closed-loop control, which is the one that has the smallest norm  $\delta^*$  in  $\delta_i, \forall i$ .
5. Shape with pre- and post-compensators the best nominal model  $G_0$ . ( $G_s = W_1 G_0 W_2$ ).
6. Design a robust controller using  $\mathcal{H}_\infty$  loop-shaping for  $G_s$  and compute  $b_{PC, \max}$ , the maximum uncertainty ball that the controller can tolerate.

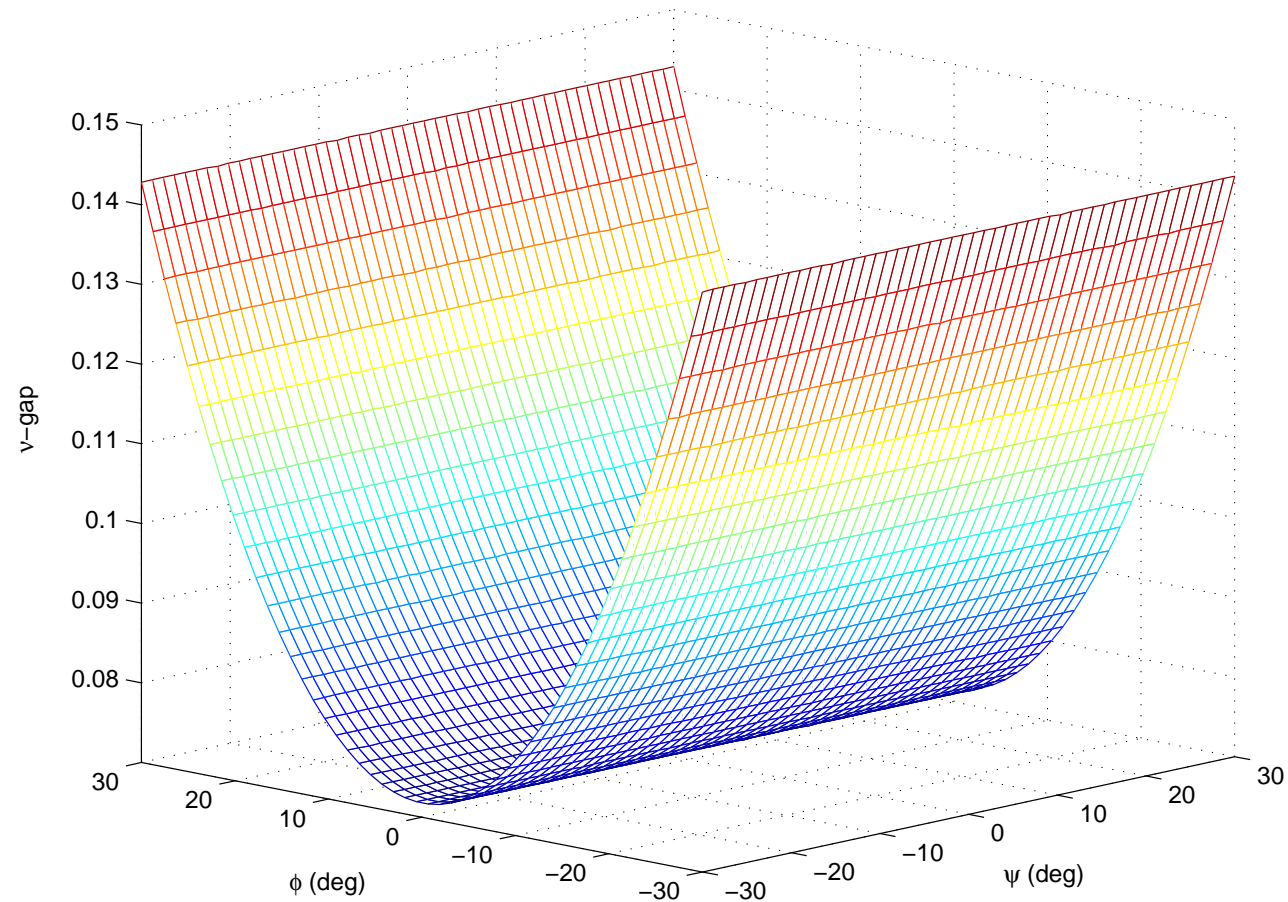
## A Computational Algorithm (II)

7. If  $b_{PC,\max}$  is small ( $b_{PC,\max} < 0.25$ ), go to step 5. (This often indicates that the chosen loop shape is incompatible with robust stability requirements).
8. Find the farthest point  $G'$  (in the  $\nu$  gap metric sense) in the polytope centered at  $G_0$ . The  $\nu$ -gap between  $G_0$  and  $G'$  is denoted by  $\delta'$ .
9. If the maximum generalized stability margin  $b_{PC,\max}$  is greater than  $\delta'$ , the nonlinearity is manageable by the designed linear controller.
10. If  $b_{PC,\max} < \delta'$ , the nonlinearity is larger than what the linear controller can cope with.

## Analysis Results (I)

- Scheduling parameters:  
yaw angle ( $\psi$ ), roll angle ( $\phi$ ) and pitch angle ( $\theta$ ).
- 50 grid points on all three scheduling parameters.
- Nominal model:  $\psi = 0^\circ$ ,  $\phi = 0^\circ$  and  $\theta = 0^\circ$ .
- The most dissimilar model:  $\psi = -25.1^\circ$ ,  $\phi = 30^\circ$  and  $\theta = 30^\circ$ .
- $\nu_{worst}\text{-gap} = 0.1429$  (between the nominal and the most dissimilar model).
- $b_{P,C} = 0.3532 > 0.1429 = \nu_{worst}\text{-gap}$
- Algorithm conclusion: **The resulting linear controller is sufficient.**

## Analysis Results (II)



Vinnicombe metric of UAV subject to  $\psi \in [-30^\circ 30^\circ]$ ,  $\phi \in [-30^\circ 30^\circ]$  at  $\theta = 30^\circ$

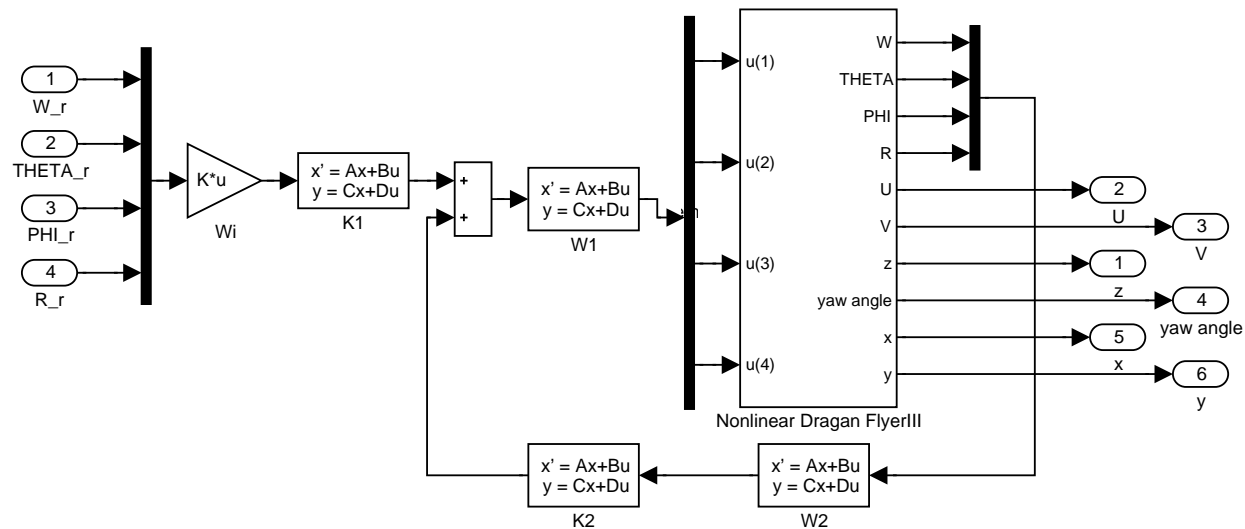
## 2 DOF $H_\infty$ Loop Shaping Controller Design (I)

Advantages of the 2 DOF  $H_\infty$  loop shaping controller design method:

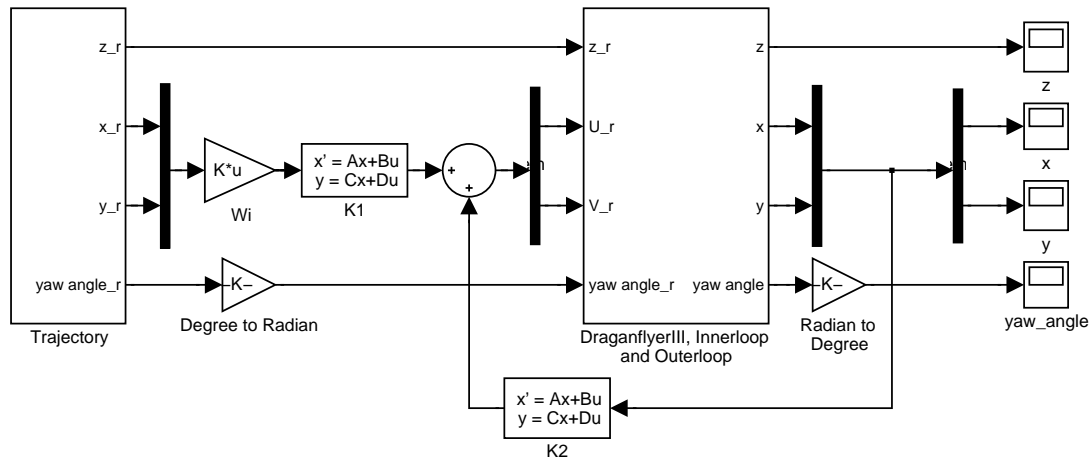
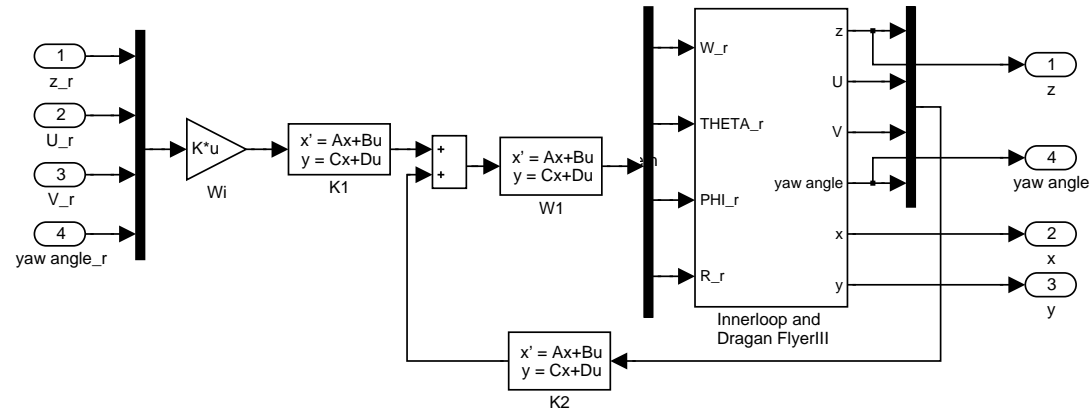
- The model can be easily tuned to a required system bandwidth.
- The generalized stability margin  $\varepsilon$  ensures the robust stability.
- Large coprime factor type model uncertainty is allowed.
- The controller gain scheduling and anti-windup can be easily addressed within the  $H_\infty$  loop shaping framework.
- The two degree of freedom structure guarantees the good reference tracking and disturbance rejection.

## 2 DOF $H_\infty$ Loop Shaping Controller Design (II)

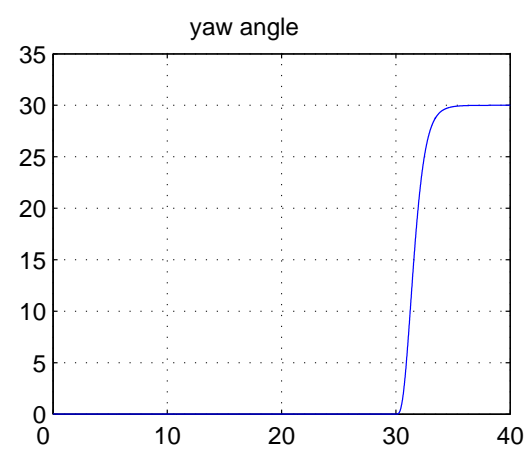
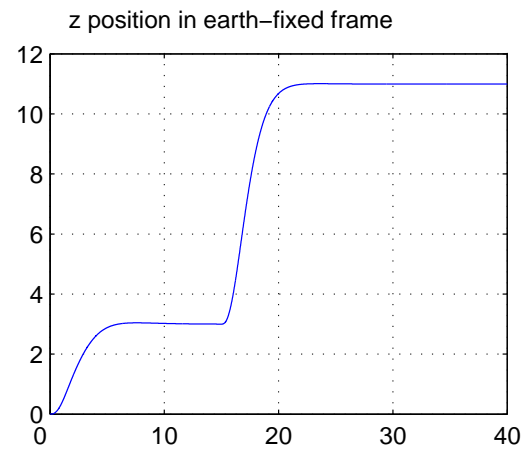
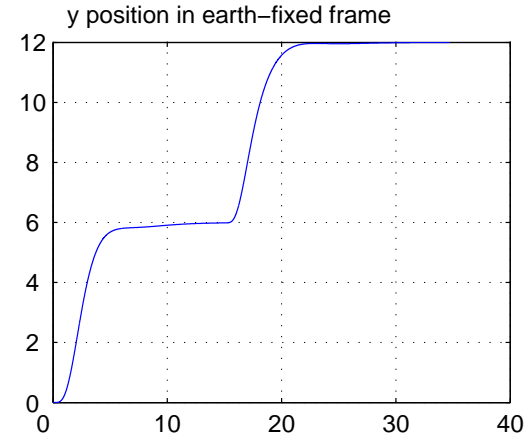
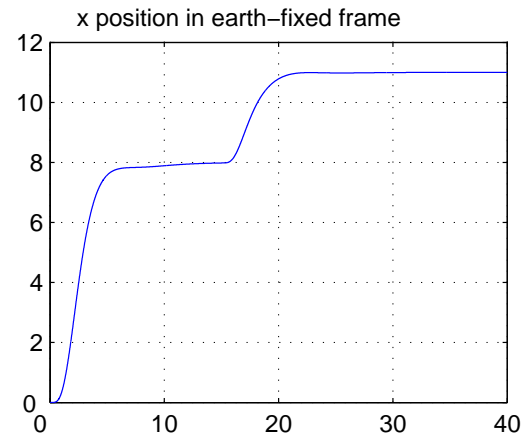
- The controller architecture includes one inner loop and two outer loops.
- The inner loop shown below provides hover control and decoupling of the nonlinear system.
- The outer loops provide velocity and trajectory control.



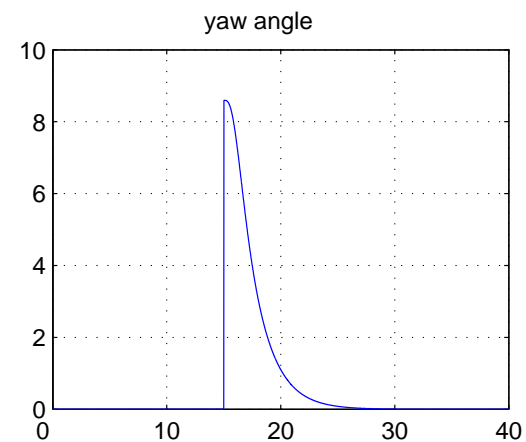
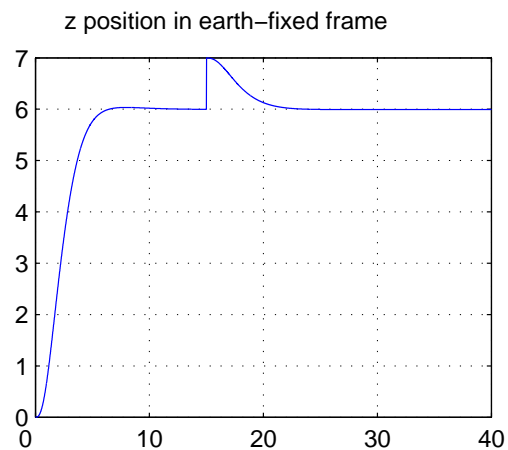
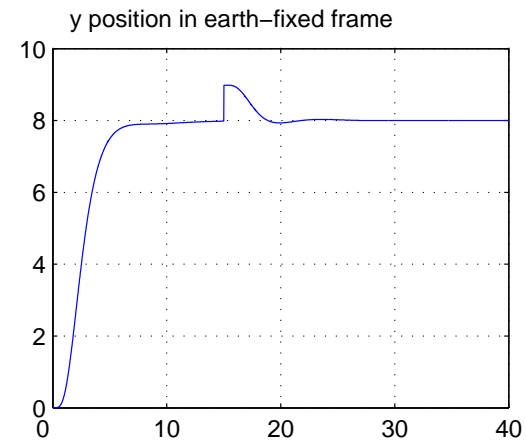
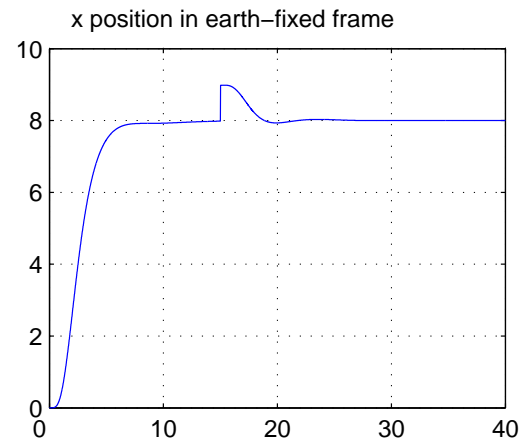
## 2 DOF $H_\infty$ Loop Shaping Controller Outer loops



## Trajectory Simulation of the Nonlinear Model With the 2 DOF $H_\infty$ Flight Controller



## Output Step Disturbance Responses With the 2 DOF $H_\infty$ Flight Controller



## Conclusions

- An UAV rig has been designed and instrumented.
- Nonlinear modelling and identification produced a high fidelity model for low speeds.
- Quasi-LPV transformation facilitates controller design, analysis and implementation.
- Analytical plant nonlinearity measures have been developed and used with success.
- A complete 2DOF Hinf controller design performs well navigation, guidance and stability augmentation tasks.

## Future Work

- Expand the UAV rig to accommodate longer flying range (power and wireless communication).
- Reconfigurable control in case of failures (DC motors, gears or blades).
- High fidelity nonlinear modelling for high speeds.
- Formation flying and cooperative control with four such UAVs.

**Topic related, accepted and submitted, publications:**

- "A combined MBPC/2 DOF Hinf controller for quad rotor unmanned air vehicle", M. Cheng, M. Huzmezan, AIAA Atmospheric Flight Mechanics Conference and Exhibit, Austin, Texas, USA, August 11–14, 2003
- "A simulation model and Hinf loopshaping control of a quad rotor unmanned air vehicle", M. Cheng, M. Huzmezan, Modelling and Simulation Conference, Palm Springs, California, USA, Feb 24–26, 2003
- "Vinnicombe metric as a nonlinearity measure", G.T. Tan, M Huzmezan and K.E. Kwook European Control Conference, Cambridge, UK September 1–4, 2003
- "Advances on measuring the closed-loop nonlinearity: A Vinnicombe Metric Approach", G.T. Tan, M Huzmezan and K.E. Kwook, Control and Decision Conference Maui, Hawaii, USA, December 9-12, 2003

**Individual grants applied for:**

- Nonlinearity Measures for Quasi-LPV Systems, NSERC Discovery, \$34,000 CAD per annum, 4 years
- Unmanned Air Vehicles From Theory to Reality, NSERC Research Tools and Instruments, \$57,760 CAD